

Bounds on the electromagnetic dipole moments through the single top production at the CLIC

M. Köksal^{*,1} A. A. Billur^{†,2} and A. Gutiérrez-Rodríguez^{‡3}

¹*Department of Optical Engineering, Cumhuriyet University, 58140, Sivas, Turkey.*

²*Department of Physics, Cumhuriyet University, 58140, Sivas, Turkey.*

³*Facultad de Física, Universidad Autónoma de Zacatecas*

Apartado Postal C-580, 98060 Zacatecas, México.

(Dated: December 3, 2024)

Abstract

We obtain bounds on the anomalous magnetic and electric dipole moments of the t -quark from a future high-energy and high-luminosity linear electron positron collider, such as the CLIC, with unpolarized and polarized electron beams which are a powerful tool to determine new physics. We consider the processes $\gamma e^- \rightarrow \bar{t} b \nu_e$ (γ is the Compton backscattering photon) and $e^+ e^- \rightarrow e^- \gamma^* e^+ \rightarrow \bar{t} b \nu_e e^+$ (γ^* is the Weizsacker-Williams photon) which are one of the most important sources of single top quark production. For a center-of-mass energy of $\sqrt{s} = 3 \text{ TeV}$, integrated luminosity of $\mathcal{L} = 2 \text{ ab}^{-1}$ and 2σ (3σ) C.L. the future $e^+ e^-$ collider may put bounds on the electromagnetic dipole moments \hat{a}_V and \hat{a}_A of the top quark of the order of 10^{-2} , which are highly competitive or even better than those recently reported in previous studies.

PACS numbers: 14.65.Ha, 13.40.Em

Keywords: Top quarks, Electric and Magnetic Moments.

* mkoksal@cumhuriyet.edu.tr

† abillur@cumhuriyet.edu.tr

‡ alexgu@fisica.uaz.edu.mx

I. INTRODUCTION

The top quark is by far the heaviest particle of the Standard Model (SM) [1–3], its mass is $m_t = 173.5 \pm 0.6$ (stat.) ± 0.8 (syst.) [4]. Up to now, the top quark has only been studied at hadron colliders, at the Tevatron and at the Large Hadron Collider (LHC). Its large mass implies that the top quark is the SM particle most strongly coupled to the mechanism of electroweak symmetry breaking. Mainly for this and other reasons, it is considered to be one of the most likely places where new physics might be discovered, which is to say, the top quark is a window to any new physics at the TeV energy scale. While enough information about the top quark is already available, showing consistency with SM expectations, its properties and interactions are among the most important measurements for present and future high energy colliders [5–8].

While the top quark has been studied in some detail at the Tevatron and LHC, many of its properties besides the mass, spin, the color and electric charges, the electric and magnetic dipole moments and the chromomagnetic and chromoelectric dipole moments are still poorly constrained. Significant new insights on top quark properties will therefore be on of the tasks of the LHC and the Compact Linear Collider (CLIC).

Some the most sensitive observable of the top quark are their dipole moments, and although these intrinsic properties have been studies extensively, both theoretically and experimentally, it is necessary to have more precise measurements on the dipole moments of the top quark.

In the SM the prediction for the Magnetic Dipole Moment (MDM) of the top quark is $a_t^{SM} = 0.02$ [9], which can be tested in the current and future colliders, which is to say, LHC and CLIC. In contrast, the Electric Dipole Moment (EDM) of the top quark is strongly suppressed and is less than 10^{-30} ecm [10–12], much too small to be observed. However, is highly attractive for probing new physics.

The sensitivity to the EDM has been studied in models with vector like multiplets, which predicted the top quark EDM close to 1.75×10^{-3} [13].

There are studies performed via the $t\bar{t}\gamma$ production for the LHC at $\sqrt{s} = 14 TeV$ and $\mathcal{L} = 300 fb^{-1}$ and $3000 fb^{-1}$, reporting the limits of ± 0.2 and ± 0.1 , respectively [14]. Other limits are reported in the literature: $-2.0 \leq \hat{a}_V \leq 0.3$ and $-0.5 \leq \hat{a}_A \leq 1.5$ which are obtained from the branching ratio and the CP asymmetry from radiative $b \rightarrow s$ transitions

[15], while the bounds of $|\hat{a}_V| < 0.05$ (0.09) and $|\hat{a}_A| < 0.20$ (0.28) comes from measurements of $\gamma e^- \rightarrow t\bar{t}$ cross section with 10% (18%) uncertainty, respectively [16]. More recent limits on the top quark magnetic and electric dipole moments at the LHC with $\sqrt{s} = 14 \text{ TeV}$, $\mathcal{L} = 3000 \text{ fb}^{-1}$ and 68% C.L. are $-0.6389 \leq \hat{a}_V \leq 0.0233$ and $|\hat{a}_A| \leq 0.1158$ [17].

Following references [14, 17–20], the definition of the general effective coupling $\gamma t\bar{t}$ including the SM coupling and contributions from dimension-six effective operators can be parameterized by the following effective Lagrangian:

$$\mathcal{L}_{\gamma t\bar{t}} = -g_e Q_t \bar{t} \Gamma_{\gamma t\bar{t}}^\mu t A_\mu, \quad (1)$$

where g_e is the electromagnetic coupling constant, Q_t is the top quark electric charge and the Lorentz-invariant vertex function $\Gamma_{\gamma t\bar{t}}^\mu$ which describes the interaction of a γ photon with two top quarks can be parameterized by

$$\Gamma_{\gamma t\bar{t}}^\mu = \gamma^\mu + \frac{i}{2m_t} (\hat{a}_V + i\hat{a}_A \gamma_5) \sigma^{\mu\nu} q_\nu, \quad (2)$$

where m_t is the mass of the top quark, q is the momentum transfer to the photon and the couplings \hat{a}_V and \hat{a}_A are real and related to the anomalous magnetic moment and the electric dipole moment of the top quark, respectively.

The linear colliders may have another option that polarized beam collisions. These type of collisions give new perspectives such as on the hadronic structure and high precision measurements on the electroweak mixing angle. Beam polarization could be important role in the next linear colliders as well as RHIC and HERA. It is expected that about 80% polarization of lepton beam can be achivable at the future linear colliders. In this work, we take into account one beam can be -80% polarization. It is worth mentioning that the polarization $P_e = -80\%$ enhances the cross sections according to the unpolarized case.

In this work we study the sensibility of the anomalous magnetic and electric dipole moments of the top quark through the processes $\gamma e^- \rightarrow \bar{t} b \nu_e$ (γ is the Compton backscattering photon) and $e^+ e^- \rightarrow e^- \gamma^* e^+ \rightarrow \bar{t} b \nu_e e^+$ (γ^* is the Weizsacker-Williams photon) which are one of the most important sources of single top quark production [21, 22]. We use center-of-mass energies of the CLIC in this work [23]. These values are for a center-of-mass energy of 1.4 TeV with integrated luminosity of 1500 fb^{-1} and 3 TeV with $\mathcal{L} = 2000 \text{ fb}^{-1}$, with unpolarized and polarized electron beams, which is to say, $P_{e^-} = -80\%$ and $P_{e^+} = 0\%$ [24].

Not only can the future e^+e^- linear collider be designed to operate in e^+e^- collision mode, but it can also be operated as a $e\gamma$ and $\gamma\gamma$ collider. This is achieved by using Compton backscattered photons in the scattering of intense laser photons on the initial e^+e^- beams. The other well-known applications of linear colliders are to study new physics beyond the SM through $e\gamma^*$ and $\gamma^*\gamma^*$ collisions. A quasireal γ^* photon emitted from one of the incoming e^- or e^+ beams can interact with the other lepton shortly after, and the subprocess $\gamma^*e^- \rightarrow \bar{t}b\nu_e$ can generate. Hence, first, we calculate the main reaction $e^+e^- \rightarrow e^-\gamma^*e^+ \rightarrow \bar{t}b\nu_e e^+$ by integrating the cross section for the subprocess $\gamma^*e^- \rightarrow \bar{t}b\nu_e$. In this case, the quasireal photons in γ^*e^- collisions can be examined by Equivalent Photon Approximation (EPA) [25–27], which is to say, by using the Weizsacker-Williams approximation (WWA). Also, we can add part related to the large values of Q_{max}^2 which do not bring an important contribution to obtain sensitivity limits on the anomalous couplings [28–31]. In EPA, photons emitted from incoming leptons which have very low virtuality are scattered at very small angles from the beam pipe and because the emitted quasireal photons have a low Q^2 virtuality these are almost real. We use only the photon virtuality of $Q_{max}^2 = 2 \text{ GeV}^2$. These processes have been observed phenomenologically and experimentally at the LEP, Tevatron and LHC [32–53].

With these motivations, we study the potential of the processes $\gamma e^- \rightarrow \bar{t}b\nu_e$ and $e^+e^- \rightarrow e^+\gamma^*e^- \rightarrow \bar{t}b\nu_e e^+$ via Compton backscattering and WWA, respectively and derive bounds on the dipole moments \hat{a}_V and \hat{a}_A at 2σ and 3σ level (90% and 95% C.L.), and at a future high-energy and high-luminosity linear electron positron collider, such as the CLIC to study the sensibility on the anomalous magnetic and electric dipole moments of the top quark.

For this we calculate the main reaction $e^+e^- \rightarrow e^-\gamma^*e^+ \rightarrow \bar{t}b\nu_e e^+$ by integrating the cross section for the subprocess $\gamma^*e^- \rightarrow \bar{t}b\nu_e$. In this case, while lepton emitted photon is not detect by central detector, the others particles are detect in the central detectors. We also present the results for the b -tagging efficiency of 0.8 and the acceptance cuts will imposed as $|\eta^b| < 2.5$ for pseudorapidity, $p_T^b > 20 \text{ GeV}$ and $p_T^{\nu_e} > 10 \text{ GeV}$ for transverse momentums of the final state particles. In addition, for this we consider hadronic decay channels of the top quark, which is to say, $BR = 0.676$ (Hadronic branching ratio). The corresponding Feynman diagrams for the main reactions as well as for the subprocesses which give the most important contribution to the total cross section are shown in Figs. 1-2.

To illustrate our results for both processes we show the dependence of the total cross section as a function of the magnetic moment and electric dipole moments \hat{a}_V and \hat{a}_A of the

top quark for two different values of the center-of-mass energies 1.4 and 3 TeV , respectively. We also include a contours plot for the upper bounds of the anomalous couplings \hat{a}_V and \hat{a}_A with 95% C.L. for different values of the center-of-mass energies $\sqrt{s} = 1.4, 3 \text{ TeV}$ with corresponding maximum luminosities for both processes. The sensitivity limits on the magnetic moment \hat{a}_V and the electric dipole moment \hat{a}_A of the top quark for some values of the center-of-mass energy and luminosity are also calculated.

This paper is organized as follows. In Section II, we study the dipole moments of the top quark through the process $\gamma e^- \rightarrow \bar{t} b \nu_e$. In Section III, we study the dipole moments of the top quark through the process $e^+ e^- \rightarrow e^+ \gamma^* e^- \rightarrow \bar{t} b \nu_e e^+$. Finally, we present our results and conclusions in Section IV.

II. COMPTON BACKSCATTERING: CROSS SECTION OF $\gamma e^- \rightarrow \bar{t} b \nu_e$

In this section we present numerical results of the cross section for the process $\gamma e^- \rightarrow \bar{t} b \nu_e$, with unpolarized and polarized electron beams, which is to say, $P_{e-} = -80\%$ and $P_{e+} = 0\%$ and as a function of the anomalous couplings of the top quark \hat{a}_V and \hat{a}_A . In addition, we presented limits contours in the plane $(\hat{a}_V - \hat{a}_A)$. We carry out the calculations using the framework of the minimally extended standard model at future linear γe^- collisions such as the CLIC.

We use the CalcHEP [54, 55] packages for calculations of the matrix elements and cross sections. These packages provide automatic computation of the cross sections and distributions in the SM as well as their extensions at tree level. We consider the high-energy stage of possible future linear γe^- collisions with $\sqrt{s} = 1.4$ and 3 TeV and design luminosity 50, 300, 500, 1000, 1500 and 2000 fb^{-1} according to the new data reported by the CLIC [23]. In addition, we consider the acceptance cuts of $|\eta^b| < 2.5$ for pseudorapidity, $p_T^b > 20 \text{ GeV}$ and $p_T^{\nu_e} > 10 \text{ GeV}$ for transverse momentum of the final state particles. We also consider the hadronic decay channels of the top quark, which is to say, $BR = 0.676$ and b -tagging efficiency of 0.8 for $\gamma e^- \rightarrow \bar{t} b \nu_e$.

A. Top quark dipole moments through the process $\gamma e^- \rightarrow \bar{t} b \nu_e$ with polarized beams

The corresponding Feynman diagrams for the main reaction $\gamma e^- \rightarrow \bar{t} b \nu_e$ that give the most important contribution to the total cross section are shown in Figs. 1-2. From Fig. 2, the Feynman diagrams (1)-(3) correspond to the contribution of the standard model, while diagram (4) corresponds to the anomalous contribution, which is to say, for the γe^- collisions there are SM background at the tree level so the total cross section is proportional to $\sigma_{Tot} = \sigma_{SM} + \sigma_{Int}(\hat{a}_V, \hat{a}_A) + \sigma_{Anom}(\hat{a}_V^2, \hat{a}_A^2, \hat{a}_V \hat{a}_A)$, respectively.

To illustrate our results we show the dependence of the cross section on the anomalous couplings \hat{a}_V and \hat{a}_A for $\gamma e^- \rightarrow \bar{t} b \nu_e$ in Fig. 3 for $P_{e^-} = -80\%$, $P_{e^+} = 0\%$ [24] and two different center-of-mass energies $\sqrt{s} = 1.4, 3 TeV$ [23], whereas the \hat{a}_V (\hat{a}_A) anomalous coupling is kept fixed at zero. We observed that the cross section is sensitive to the value of the center-of-mass energies. The sensitivity to $\bar{t} b \nu_e$ increases with the collider energy reaching a maximum at the end of the range considered: $\hat{a}_{V,A} = \pm 1$. At the end of this range, the cross section for $\sqrt{s} = 3 TeV$ increases relative to $\sqrt{s} = 1.4 TeV$ up to 24.5%. By contrast, in the vicinity of $\hat{a}_{V,A} = 0$ the total cross section is smaller. We notice that, as shown in Fig. 3, the $\gamma e^- \rightarrow \bar{t} b \nu_e$ production process at an CLIC-based γe^- collider reaches a value of $\sigma = 0.55 pb$ for $\sqrt{s} = 3 TeV$. The obvious conclusion is that in this case the $\gamma t \bar{t}$ coupling could be probed with remarkable sensitivity (see Table I).

In Fig. 4 we used two center-of-mass energies $\sqrt{s} = 1.4, 3 TeV$ planned for the CLIC accelerator in order to get contours limits in the plane $\hat{a}_V - \hat{a}_A$ for $\gamma e^- \rightarrow \bar{t} b \nu_e$ and the planned luminosities of $\mathcal{L} = 50, 300, 500, 1000, 1500, 2000 fb^{-1}$ and b - tagging efficiency = 0.8.

As an indicator of the order of magnitude, in Table I we present the bounds obtained on the \hat{a}_V magnetic moment and \hat{a}_A electric dipole moments of the t-quark with the polarization $P_{e^-} = -80\%$ for the electron beams and $P_{e^+} = 0\%$ for the positron and $\sqrt{s} = 1.4, 3 TeV$, $\mathcal{L} = 50, 300, 500, 1000, 1500, 2000 fb^{-1}$ at 2σ and $3\sigma C.L.$, respectively. As expected, our results presented in Table I clearly show that as the energy and luminosity of the collider increases, the bounds on the dipole moments of the top quark are stronger. We observed that the results obtained in Table I are competitive or even better than those recently reported in previous studies [14–17].

TABLE I: Bounds on the \hat{a}_V magnetic moment and \hat{a}_A electric dipole moment for the process $\gamma e^- \rightarrow \bar{t}b\nu_e$ (γ is the Compton backscattering photon) for $P_{e^-,e^+} = -80\%, 0\%$, b -tagging efficiency = 0.8 at 2σ and 3σ C.L.

2σ C.L.			
$\sqrt{s} (TeV)$	$\mathcal{L} (fb^{-1})$	\hat{a}_V	$ \hat{a}_A $
1.4	50	[-0.1091, 0.1565]	0.1615
1.4	300	[-0.0630, 0.1103]	0.1032
1.4	500	[-0.0534, 0.1007]	0.0908
1.4	1000	[-0.0424, 0.0897]	0.0763
1.4	1500	[-0.0369, 0.0842]	0.0689
3	50	[-0.0724, 0.0816]	0.0768
3	300	[-0.0447, 0.0539]	0.0491
3	500	[-0.0389, 0.0480]	0.0432
3	1000	[-0.0320, 0.0412]	0.0364
3	1500	[-0.0286, 0.0377]	0.0329
3	2000	[-0.0234, 0.0325]	0.0277
3σ C.L.			
1.4	50	[-0.1209, 0.1683]	0.1762
1.4	300	[-0.0703, 0.1177]	0.1126
1.4	500	[-0.0598, 0.1071]	0.0990
1.4	1000	[-0.0477, 0.0950]	0.0833
1.4	1500	[-0.0416, 0.0889]	0.0752
3	50	[-0.0794, 0.0886]	0.0838
3	300	[-0.0492, 0.0583]	0.0535
3	500	[-0.0428, 0.0520]	0.0472
3	1000	[-0.0353, 0.0445]	0.0396
3	1500	[-0.0315, 0.0407]	0.0358
3	2000	[-0.0258, 0.0350]	0.0301

B. Top quark dipole moments through the process $\gamma e^- \rightarrow \bar{t} b \nu_e$ with unpolarized beams

Following a similar procedure as in subsection A, we show our results for the total cross section on the anomalous couplings \hat{a}_V and \hat{a}_A for the process $\gamma e^- \rightarrow \bar{t} b \nu_e$ with unpolarized beams, which is one of the most important sources of single top quark production. In Fig. 5, our results are presented for two different center-of-mass energies $\sqrt{s} = 1.4, 3 \text{ TeV}$. The cross section for $\gamma e^- \rightarrow \bar{t} b \nu_e$ is sensitive to the value of the center-of-mass energies and this sensitivity to $\bar{t} b \nu_e$ increases with the collider energy reaching a maximum at the end of the range considered, which is to say, $\hat{a}_{V,A} = \pm 1$. Comparing the curves in Fig. 5, we see that the sensitivity of the cross section for the center-of-mass energies of $\sqrt{s} = 1.4$ and 3 TeV increases up to 26.6% at the ends of the interval considered. The opposite effect is observed in the vicinity of $\hat{a}_{V,A} = 0$ where the cross section is smaller. We notice that, as shown in Fig. 5, the $\gamma e^- \rightarrow \bar{t} b \nu_e$ production process at an CLIC-based γe^- collider reaches a value of $\sigma = 0.3 \text{ pb}$ for $\sqrt{s} = 3 \text{ TeV}$. The evident conclusion is that in this case the $\gamma t\bar{t}$ coupling could be probed with remarkable sensitivity (see Table II).

In Fig. 6 we used two center-of-mass energies $\sqrt{s} = 1.4, 3 \text{ TeV}$ planned for the CLIC accelerator in order to get contours limits in the plane $\hat{a}_V - \hat{a}_A$ for $\gamma e^- \rightarrow \bar{t} b \nu_e$ with the planned luminosities of $\mathcal{L} = 50, 300, 500, 1000, 1500, 2000 \text{ fb}^{-1}$ and b -tagging efficiency = 0.8.

In Table II we present the bounds obtained on the \hat{a}_V magnetic moment and \hat{a}_A electric dipole moments of the top quark for $\sqrt{s} = 1.4, 3 \text{ TeV}$ and $\mathcal{L} = 50, 300, 500, 1000, 1500, 2000 \text{ fb}^{-1}$ at 2σ and $3\sigma \text{ C.L.}$, respectively. The final value adopted for the center-of-mass energy of $\sqrt{s} = 3 \text{ TeV}$ and the integrated luminosity of $\mathcal{L} = 2 \text{ ab}^{-1}$ at 2σ and 3σ , is the most sensitive interval to the \hat{a}_V (\hat{a}_A). Increasing the \sqrt{s} as well as the \mathcal{L} provide more restricted bounds on both the anomalous couplings \hat{a}_V and \hat{a}_A . We observed that the results obtained in Table II are competitive or even better than those recently reported in previous studies [14–17].

Comparison of Tables I and II clearly shows that the effects of the polarized electron beams $P_{e^-,e^+} = -80\%, 0\%$ enhances the total cross section as well as improving the bounds on the dipole moments of the top quark, according to the unpolarized beams case.

TABLE II: Bounds on the \hat{a}_V magnetic moment and \hat{a}_A electric dipole moment for the process $\gamma e^- \rightarrow \bar{t} b \nu_e$ (γ is the Compton backscattering photon) for b – tagging efficiency = 0.8 at 2σ and 3σ C.L.

2σ C.L.			
$\sqrt{s} (TeV)$	$\mathcal{L} (fb^{-1})$	\hat{a}_V	$ \hat{a}_A $
1.4	50	[-0.1624, 0.2158]	0.1872
1.4	300	[-0.0958, 0.1493]	0.1196
1.4	500	[-0.0882, 0.1353]	0.1052
1.4	1000	[-0.0657, 0.1192]	0.0885
1.4	1500	[-0.0576, 0.1111]	0.0800
3	50	[-0.0845, 0.0936]	0.0887
3	300	[-0.0523, 0.0614]	0.0563
3	500	[-0.0454, 0.0545]	0.0494
3	1000	[-0.0375, 0.0465]	0.0414
3	1500	[-0.0334, 0.0425]	0.0373
3	2000	[-0.0273, 0.0364]	0.0312
3σ C.L.			
1.4	50	[-0.1793, 0.2327]	0.2043
1.4	300	[-0.1065, 0.1599]	0.1305
1.4	500	[-0.0912, 0.1447]	0.1149
1.4	1000	[-0.0735, 0.1269]	0.0969
1.4	1500	[-0.0645, 0.1180]	0.0873
3	50	[-0.0926, 0.1017]	0.0966
3	300	[-0.0574, 0.0665]	0.0616
3	500	[-0.0500, 0.0591]	0.0541
3	1000	[-0.0413, 0.0504]	0.0453
3	1500	[-0.0368, 0.0459]	0.0408
3	2000	[-0.0301, 0.0392]	0.0341

III. WEIZSACKER-WILLIAMS APPROXIMATION: CROSS SECTION OF

$$e^+e^- \rightarrow e^+\gamma^*e^- \rightarrow \bar{t}b\nu_e e^+$$

In this section we study the dipole moments of the top quark via the process $e^+e^- \rightarrow e^+\gamma^*e^- \rightarrow \bar{t}b\nu_e e^+$, with unpolarized and polarized e^- beams and for the new center-of-mass energies of the CLIC [23].

A. Top quark dipole moments through the process $e^+e^- \rightarrow e^+\gamma^*e^- \rightarrow \bar{t}b\nu_e e^+$ with polarized beams

The corresponding Feynman diagrams for the subprocess $\gamma^*e^- \rightarrow \bar{t}b\nu_e$ that give the most important contribution to the total cross section are shown in Figs. 1-2. In this case, the total cross section of the subprocess depends of the contribution of the standard model, which is to say, on the diagrams (1)-(3) and on the diagram (4) with anomalous couplings, such that, $\sigma_{Tot} = \sigma_{SM} + \sigma_{Int}(\hat{a}_V, \hat{a}_A) + \sigma_{Anom}(\hat{a}_V^2, \hat{a}_A^2, \hat{a}_V\hat{a}_A)$.

For the study of the process $e^+e^- \rightarrow e^+\gamma^*e^- \rightarrow \bar{t}b\nu_e e^+$ in Fig. 7, we show the total cross section as a function of the electromagnetic form factors of the top quark \hat{a}_V and \hat{a}_A for $P_{e^-,e^+} = -80\%, 0\%$ [24], two different center-of-mass energies $\sqrt{s} = 1.4, 3 TeV$ [23] and the Weizsacker-Williams photon virtuality $Q^2 = 2 GeV^2$ [28–31], respectively. We can see from this figure that the total cross section changes strongly with the variation of the \sqrt{s} values and this variation is of the order 20% at the ends of the range considered to \hat{a}_V and \hat{a}_A , which is to say, $\hat{a}_{V,A} = \pm 1$.

In Fig. 8 we summarize the respective limit contours for the dipole moments in the $(\hat{a}_V - \hat{a}_A)$ plane for the process $e^+e^- \rightarrow e^+\gamma^*e^- \rightarrow \bar{t}b\nu_e e^+$. The curves are for $\sqrt{s} = 1.4 TeV$, $\mathcal{L} = 50, 500, 1500 fb^{-1}$ and $\sqrt{s} = 3 TeV$, $\mathcal{L} = 50, 500, 2000 fb^{-1}$, respectively. We have used $Q^2 = 2 GeV^2$ and b – tagging efficiency = 0.8.

We determined the values numerical of the bounds obtained on the \hat{a}_V magnetic moment and \hat{a}_A electric dipole moment for $\sqrt{s} = 1.4, 3 TeV$, $Q^2 = 2 GeV^2$, and $\mathcal{L} = 50, 300, 500, 1000, 1500, 2000 fb^{-1}$ at 2σ and 3σ in Table III. We observed that the results obtained in Table III are competitive with the bounds reported in the literature [14–17].

TABLE III: Bounds on the \hat{a}_V magnetic moment and \hat{a}_A electric dipole moment for the process $e^+e^- \rightarrow e^+\gamma^*e^- \rightarrow \bar{t}b\nu_e e^+$ (γ^* is the Weizsacker-Williams photon) for $Q^2 = 2 \text{ GeV}^2$, $P_{e^-,e^+} = -80\%, 0\%$, b - tagging efficiency = 0.8 at 2σ and 3σ C.L.

2σ C.L.			
$\sqrt{s} \text{ (TeV)}$	$\mathcal{L} \text{ (fb}^{-1}\text{)}$	\hat{a}_V	$ \hat{a}_A $
1.4	50	[-0.3474, 0.4397]	0.3908
1.4	300	[-0.2078, 0.3001]	0.2497
1.4	500	[-0.1784, 0.2707]	0.2197
1.4	1000	[-0.1443, 0.2366]	0.1848
1.4	1500	[-0.1271, 0.2194]	0.1670
3	50	[-0.1806, 0.2180]	0.1984
3	300	[-0.1094, 0.1469]	0.1267
3	500	[-0.0944, 0.1318]	0.1115
3	1000	[-0.0769, 0.1144]	0.0937
3	1500	[-0.0681, 0.1055]	0.0847
3	2000	[-0.0547, 0.0921]	0.0713
3σ C.L.			
1.4	50	[-0.3827, 0.4750]	0.4264
1.4	300	[-0.2302, 0.3225]	0.2724
1.4	500	[-0.1980, 0.2903]	0.2397
1.4	1000	[-0.1607, 0.2530]	0.2016
1.4	1500	[-0.1418, 0.2341]	0.1822
3	50	[-0.1986, 0.2360]	0.2165
3	300	[-0.1208, 0.1583]	0.1383
3	500	[-0.1044, 0.1419]	0.1217
3	1000	[-0.0853, 0.1228]	0.1023
3	1500	[-0.0756, 0.1131]	0.0924
3	2000	[-0.0609, 0.1081]	0.0777

B. Top quark dipole moments through the process $e^+e^- \rightarrow e^+\gamma^*e^- \rightarrow \bar{t}b\nu_e e^+$ with unpolarized beams

As in the previous subsections, in this study, we search for $e^+e^- \rightarrow e^+\gamma^*e^- \rightarrow \bar{t}b\nu_e e^+$ process to investigate $\gamma t\bar{t}$ anomalous couplings, for this we present the cross section as a function of the anomalous couplings \hat{a}_V and \hat{a}_A for $e^+e^- \rightarrow e^+\gamma^*e^- \rightarrow \bar{t}b\nu_e e^+$ in Fig. 9 for two different center-of-mass energies $\sqrt{s} = 1.4, 3 \text{ TeV}$ and $Q^2 = 2 \text{ GeV}^2$ [28–31]. From this figure is clear that the cross section is sensitive to the value of the center-of-mass energies and this sensitivity to $\bar{t}b\nu_e e^+$ increases with the collider energy reaching a maximum at the end of the range considered, which is to say, $\hat{a}_{V,A} = \pm 1$. This variation of the cross section for $\sqrt{s} = 1.4$ and 3 TeV is of the order 23%.

The resolving power of CLIC in the 2-dimensional space of \hat{a}_V and \hat{a}_A is shown in Fig. 10 for $e^+e^- \rightarrow e^+\gamma^*e^- \rightarrow \bar{t}b\nu_e e^+$, where \hat{a}_V and \hat{a}_A are the anomalous magnetic and electric and electric dipole moments of the t -quark. We consider the center-of-mass energies $\sqrt{s} = 1.4, 3 \text{ TeV}$ and the luminosities of $\mathcal{L} = 50, 300, 500, 1000, 1500, 2000 \text{ fb}^{-1}$ planned for the CLIC accelerator, with Weizsacker-Williams photon virtuality $Q^2 = 2 \text{ GeV}^2$ and b – tagging efficiency = 0.8.

Finally, Table IV summarizes our results on the limits to the dipole moments of the top quark and for different values of the center-of-mass energy $\sqrt{s} = 1.4, 3 \text{ TeV}$ and luminosity $\mathcal{L} = 50, 300, 500, 1000, 1500, 2000 \text{ fb}^{-1}$, we consider Weizsacker-Williams photon virtuality $Q^2 = 2 \text{ GeV}^2$ and b – tagging efficiency = 0.8. This table also lists the measurement on the dipole moments \hat{a}_V and \hat{a}_A obtained at 2σ and 3σ C.L., respectively. The limits obtained on the dipole moments through the $e^+e^- \rightarrow e^+\gamma^*e^- \rightarrow \bar{t}b\nu_e e^+$ single top quark production are competitive with the current limits, reported in the literature [14–17].

IV. CONCLUSIONS

Even though γe^- and $\gamma\gamma$ processes require new equipment, γ^*e^- and $\gamma^*\gamma^*$ are realized spontaneously at linear colliders without any equipment. These processes will allow the future linear colliders to operate in two different modes, γ^*e^- and $\gamma^*\gamma^*$, opening up the opportunity for a wider search for new physics. Therefore, the γ^*e^- linear collisions represent an excellent opportunity to study the sensibility on the anomalous magnetic moment and

TABLE IV: Bounds on the \hat{a}_V magnetic moment and \hat{a}_A electric dipole moment for the process $e^+e^- \rightarrow e^+\gamma^*e^- \rightarrow \bar{t}b\nu_e e^+$ (γ^* is the Weizsacker-Williams photon) for $Q^2 = 2 \text{ GeV}^2$, b -tagging efficiency = 0.8 at 2σ and 3σ C.L.

2σ C.L.			
$\sqrt{s} (TeV)$	$\mathcal{L} (fb^{-1})$	\hat{a}_V	$ \hat{a}_A $
1.4	50	[-0.4088, 0.5012]	0.4527
1.4	300	[-0.2467, 0.3390]	0.2892
1.4	500	[-0.2126, 0.0304]	0.2545
1.4	1000	[-0.1728, 0.2651]	0.2140
1.4	1500	[-0.1527, 0.2450]	0.1934
3	50	[-0.2126, 0.2493]	0.2299
3	300	[-0.1300, 0.1666]	0.1468
3	500	[-0.1125, 0.1491]	0.1293
3	1000	[-0.0921, 0.1287]	0.1086
3	1500	[-0.0818, 0.1184]	0.0982
3	2000	[-0.0662, 0.1028]	0.0826
3σ C.L.			
1.4	50	[-0.4499, 0.5422]	0.4938
1.4	300	[-0.2727, 0.3651]	0.3155
1.4	500	[-0.2354, 0.3277]	0.2777
1.4	1000	[-0.1919, 0.2842]	0.2335
1.4	1500	[-0.1698, 0.2622]	0.2111
3	50	[-0.2335, 0.2702]	0.2508
3	300	[-0.1433, 0.1799]	0.1602
3	500	[-0.1242, 0.1607]	0.1410
3	1000	[-0.1019, 0.1385]	0.1185
3	1500	[-0.0906, 0.1272]	0.1071
3	2000	[-0.0736, 0.1102]	0.0901

electric dipole moment of the top quark.

We have done a study of the total cross section of the processes $\gamma e^- \rightarrow \bar{t} b \nu_e$ and $e^+ e^- \rightarrow e^+ \gamma^* e^- \rightarrow \bar{t} b \nu_e e^+$, with polarized and unpolarized and electron beams as a function of the anomalous couplings \hat{a}_V and \hat{a}_A . The analysis is shown in Figs. 3, 5, and 7, 9 with Compton backscattering photon and Weizsacker-Williams photon virtuality of $Q^2 = 2 \text{ GeV}^2$, b -tagging efficiency = 0.8, respectively. In both processes, the cross section shows a strong dependence on the anomalous couplings \hat{a}_V and \hat{a}_A , as well as with the center-of-mass energy \sqrt{s} . This variation of the cross section for $\sqrt{s} = 1.4, 3 \text{ TeV}$ is of the order 24.5%, 26.6% and 20%, 23% for $\gamma e^- \rightarrow \bar{t} b \nu_e$ and $e^+ e^- \rightarrow e^+ \gamma^* e^- \rightarrow \bar{t} b \nu_e e^+$, respectively.

We also include contours plots for the dipole moments at the 95% *C.L.* in the $(\hat{a}_V - \hat{a}_A)$ plane for the processes $\gamma e^- \rightarrow \bar{t} b \nu_e$ and $e^+ e^- \rightarrow e^+ \gamma^* e^- \rightarrow \bar{t} b \nu_e e^+$ for $Q^2 = 2 \text{ GeV}^2$ and $\sqrt{s} = 1.4, 3 \text{ TeV}$ in Figures 4, 6 and 8, 10. The contours are consistent with the results obtained in Tables I-IV. From these tables we observe a strong correlation between the center-of-mass energy \sqrt{s} , integrated luminosity \mathcal{L} and the dipole moments \hat{a}_V and \hat{a}_A .

It is worth mentioning that our bounds obtained in Tables I-IV on the anomalous magnetic moment for the processes $\gamma e^- \rightarrow \bar{t} b \nu_e$ and $e^+ e^- \rightarrow e^+ \gamma^* e^- \rightarrow \bar{t} b \nu_e e^+$ for $Q^2 = 2 \text{ GeV}^2$, $\sqrt{s} = 1.4, 3 \text{ TeV}$ and $\mathcal{L} = 50, 300, 500, 1000, 1500, 2000 \text{ fb}^{-1}$ at 2σ and 3σ C.L. are competitive or even better than those recently reported in the literature [14–17].

Others promising production modes for studying the cross section and the electromagnetic dipole moments \hat{a}_V and \hat{a}_A of the top quark is through the processes $\gamma\gamma \rightarrow t\bar{t}$ (Compton backscattering photon), $\gamma^*\gamma^* \rightarrow t\bar{t}$ (Weizsacker-Williams photon) and $\gamma\gamma^* \rightarrow t\bar{t}$ (Compton backscattering photon, Weizsacker-Williams photon), respectively [56]. These processes are one of the most important sources of $t\bar{t}$ pair production.

In conclusion, we have found that the processes $\gamma e^- \rightarrow \bar{t} b \nu_e$ and $e^+ e^- \rightarrow e^+ \gamma^* e^- \rightarrow \bar{t} b \nu_e e^+$ in the γe^- and $\gamma^* e^-$ collision modes at the high energies and luminosities expected at the CLIC can be used to probe for bounds on the magnetic moment \hat{a}_V and electric dipole moment \hat{a}_A of the top quark. In particular, we can appreciate that for integrated luminosities of 2 ab^{-1} and center-of-mass energies of 3 TeV , we derive bounds on the dipole moments at 2σ and 3σ (90% and 95%) C.L.: $-0.0234 (-0.0258) \leq \hat{a}_V \leq 0.0325 (0.0350)$, $|\hat{a}_A| = 0.0277 (0.0301)$ and $-0.0273 (-0.0301) \leq \hat{a}_V \leq 0.0364 (0.0392)$, $|\hat{a}_A| = 0.0312 (0.0341)$ for $\gamma e^- \rightarrow \bar{t} b \nu_e$ with unpolarized and polarized e^- beams and of $-0.0547 (-0.0609) \leq \hat{a}_V \leq 0.0921 (0.1081)$, $|\hat{a}_A| = 0.0713 (0.0777)$ and $-0.0662 (-0.0736) \leq \hat{a}_V \leq 0.1028 (0.1102)$,

$|\hat{a}_A| = 0.0826$ (0.0901) for $e^+e^- \rightarrow e^+\gamma^*e^- \rightarrow \bar{t}b\nu_e e^+$ with unpolarized and polarized electron beams, which are highly competitive or even better than those recently reported in previous studies.

Acknowledgments

A. G. R. acknowledges support from CONACyT, SNI and PROFOCIE (México).

-
- [1] S. L. Glashow, *Nucl. Phys.* **22**, 579 (1961).
 - [2] S. Weinberg, *Phys. Rev. Lett.* **19**, 1264 (1967).
 - [3] A. Salam, in *Elementary Particle Theory*, Ed. N. Svartholm (Almqvist and Wiskell, Stockholm, 1968) 367.
 - [4] K. A. Olive, *et al.*, [Particle Data Group], *Chin. Phys.* **C38**, 090001 (2014).
 - [5] T. Abe, *et al.* [Am. LC Group], arXiv:hep-ex/0106057; G. Aarons, *et al.*, [ILC Collaboration], arXiv: 0709.1893 [hep-ph]; J. Brau, *et al.*, [ILC Collaboration], arXiv:0712.1950 [physics.acc-ph]; H. Baer, T. Barklow, K. Fujii, *et al.*, arXiv:1306.6352 [hep-ph].
 - [6] E. Accomando, *et al.* (CLIC Phys. Working Group Collaboration), arXiv: hep-ph/0412251, CERN-2004-005; D. Dannheim, P. Lebrun, L. Linssen, *et al.*, arXiv:1208.1402 [hep-ex].
 - [7] ATLAS Collaboration, *Measurement of the inclusive $t\bar{t}\gamma$ cross section with the ATLAS detector*, Tech. Rep. ATLAS-CONF-2011-153, ATLAS-COM-CONF-2011-186, 2011.
 - [8] CMS Collaboration, *Measurement of the inclusive top-quark pair + photon production cross section in the muon + jets channel in pp collisions at 8 TeV*, Tech. Rep. CMS-PAS-TOP-13-011, 2014.
 - [9] W. Bernreuther, R. Bonciani, T. Gehrmann, R. Heinesch, T. Leineweber, P. Mastrolia, E. Remiddi, *Phys. Rev. Lett.* **95**, 261802 (2005).
 - [10] A. Soni and R. M. Xu, *Phys. Rev. Lett.* **69**, 33 (1992).

- [11] M. E. Pospelov and I. B. Khriplovich, *Sov. J. Nucl. Phys.* **53**, 638 (1991) [*Yad. Fiz.* 53 (1991) 1030].
- [12] F. Hoogeveen, *Nucl. Phys.* **B341**, 322 (1990).
- [13] T. Ibrahim and P. Nath, *Phys. Rev.* **D82**, 055001 (2010).
- [14] U. Baur, A. Juste, L. H. Orr and D. Rainwater, *Phys. Rev.* **D71**, 054013 (2005).
- [15] A. O. Bouzas and F. Larios, *Phys. Rev.* **D87**, 074015 (2013).
- [16] A. O. Bouzas and F. Larios, *Phys. Rev.* **D88**, 094007 (2013).
- [17] Sh. Fayazbakhsh, S. Taheri Monfared and M. Mohammadi Najafabadi, *Phys. Rev.* **D92**, 014006 (2015).
- [18] J. F. Kamenik, M. Papucci and A. Weiler, *Phys. Rev.* **D85**, 071501 (2012).
- [19] J. A. Aguilar-Saavedra, *Nucl. Phys.* **B812**, 181 (2009).
- [20] J. A. Aguilar-Saavedra, M. C. N. Fiolhais and A. Onofre, *JHEP* **07**, 180 (2012).
- [21] E. Boos, M. Dubinin, A. Pukhov, M. Sachwitz and H. J. Schreiber, *Eur. Phys. J.* **C21**, 81 (2001).
- [22] E. Boos and L. Dudko, *Int. J. Mod. Phys.* **A27**, 1230026 (2012).
- [23] H. Abramowicz, *et al.*, The CLIC Detector and Physics Study, arXiv:1307.5288 [hep-ex].
- [24] G. Moortgat-Pick, *et al.*, *Physics Reports* **460**, 131243 (2008).
- [25] G. Baur, *et al.*, *Phys. Rep.* **364**, 359 (2002).
- [26] V. M. Budnev, I. F. Ginzburg, G. V. Meledin and V. G. Serbo, *Phys. Rep.* **15**, 181 (1975).
- [27] K. Piotrkowski, *Phys. Rev.* **D63**, 071502 (2001).
- [28] M. Acciarri, *et al.*, [L3 Collaboration], *Phys. Lett.* **B434**, 169 (1998).
- [29] K. Ackerstaff, *et al.*, [OPAL Collaboration], *Phys. Lett.* **B431**, 188 (1998).
- [30] I. Sahin, *Phys. Rev.* **D85**, 033002 (2012).
- [31] A. A. Billur, *et al.*, *Phys. Rev.* **D89**, 037301 (2014).
- [32] A. Abulencia, *et al.*, [CDF Collaboration], *Phys. Rev. Lett.* **98**, 112001 (2007).
- [33] T. Aaltonen, *et al.*, [CDF Collaboration], *Phys. Rev. Lett.* **102**, 222002 (2009).
- [34] T. Aaltonen, *et al.*, [CDF Collaboration], *Phys. Rev. Lett.* **102**, 242001 (2009).
- [35] S. Chatrchyan, *et al.*, [CMS Collaboration], *JHEP* **1201**, 052 (2012).
- [36] S. Chatrchyan, *et al.*, [CMS Collaboration], *JHEP* **1211**, 080 (2012).
- [37] V. M. Abazov, *et al.*, [D0 Collaboration], *Phys. Rev.* **D88**, 012005 (2013).
- [38] S. Chatrchyan, *et al.*, [CMS Collaboration], *JHEP* **07**, 116 (2013).

- [39] S. C. Inan, *Phys. Rev.* **D81**, 115002 (2010).
- [40] S. C. Inan, *Nucl. Phys.* **B897**, 289 (2015).
- [41] S. C. Inan, *Int. J. Mod. Phys.* **A26**, 3605 (2011).
- [42] I. Sahin and S. C. Inan, *JHEP* **0909**, 069 (2009).
- [43] S. Atag, S. C. Inan and I. Sahin, *JHEP* **1009**, 042 (2010).
- [44] I. Sahin and B. Sahin, *Phys. Rev.* **D86**, 115001 (2012).
- [45] B. Sahin and A. A. Billur, *Phys. Rev.* **D86**, 074026 (2012).
- [46] A. Senol, *Int. J. Mod. Phys.* **A29**, 1450148 (2014).
- [47] A. Senol, *Phys. Rev.* **D87**, 073003 (2013).
- [48] S. Fichtel, G. von Gersdorff, B. Lenzi, C. Royon and M. Saimpert, *JHEP* **1502**, 165 (2015).
- [49] H. Sun, *Phys. Rev.* **D90**, 035018 (2014).
- [50] H. Sun, *Nucl. Phys.* **B886**, 691 (2014).
- [51] H. Sun, Y. J. Zhou and H. S. Hou, *JHEP* **1502**, 064 (2015).
- [52] A. Senol and M. Koksall, *JHEP* **1503**, 139 (2015).
- [53] S. Atag and A. A. Billur, *JHEP* **1011**, 060 (2010).
- [54] A. Belyaev, N. D. Christensen and A. Pukhov, *Comput. Phys. Commun.* **184**, 1729 (2013).
- [55] A. Pukhov, *et al.*, CalcHEP a package for evaluation of Feynman diagrams and integration over multiparticle phase space, Report No. INP MSU 98-41/542, arXiv:hep-ph/9908288; arXiv:hep-ph/0412191.
- [56] M. Köksal, A. A. Billur and A. Gutiérrez-Rodríguez, Work in progress.

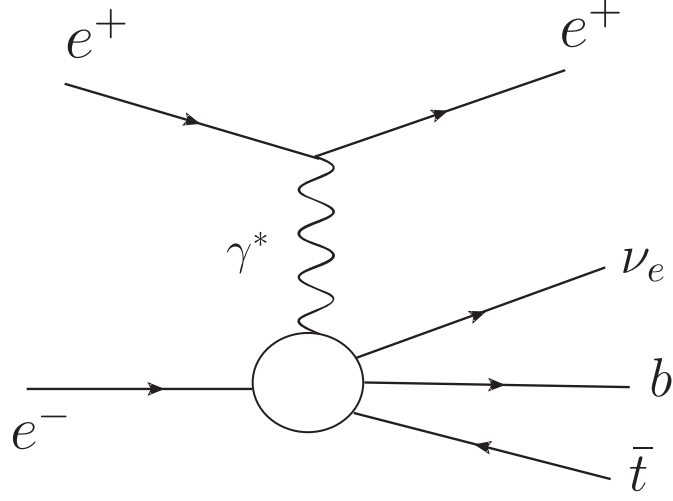


FIG. 1: Schematic diagram for the process of single top quark production $e^+e^- \rightarrow e^+\gamma^*e^- \rightarrow \bar{t}b\nu_e e^+$.

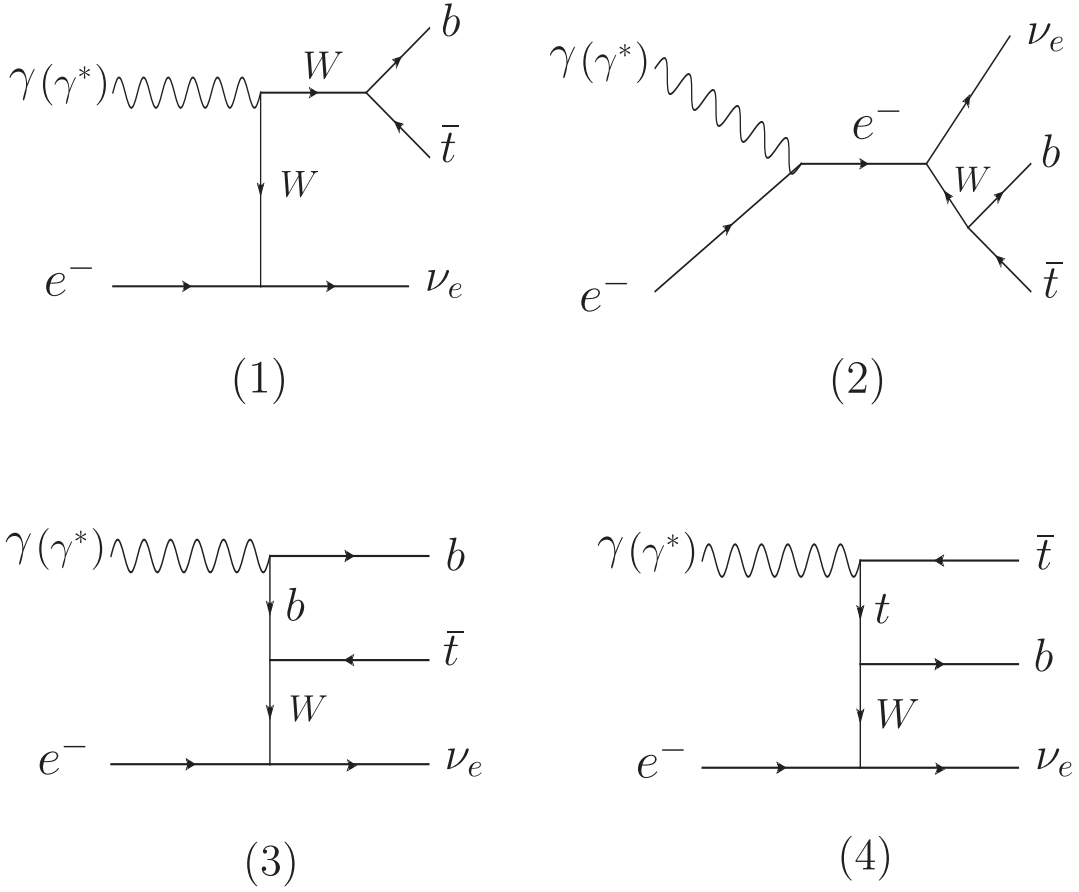


FIG. 2: The Feynman diagrams contributing to the subprocesses $\gamma e^- \rightarrow \bar{t}b\nu_e$ and $\gamma^* e^- \rightarrow \bar{t}b\nu_e$.

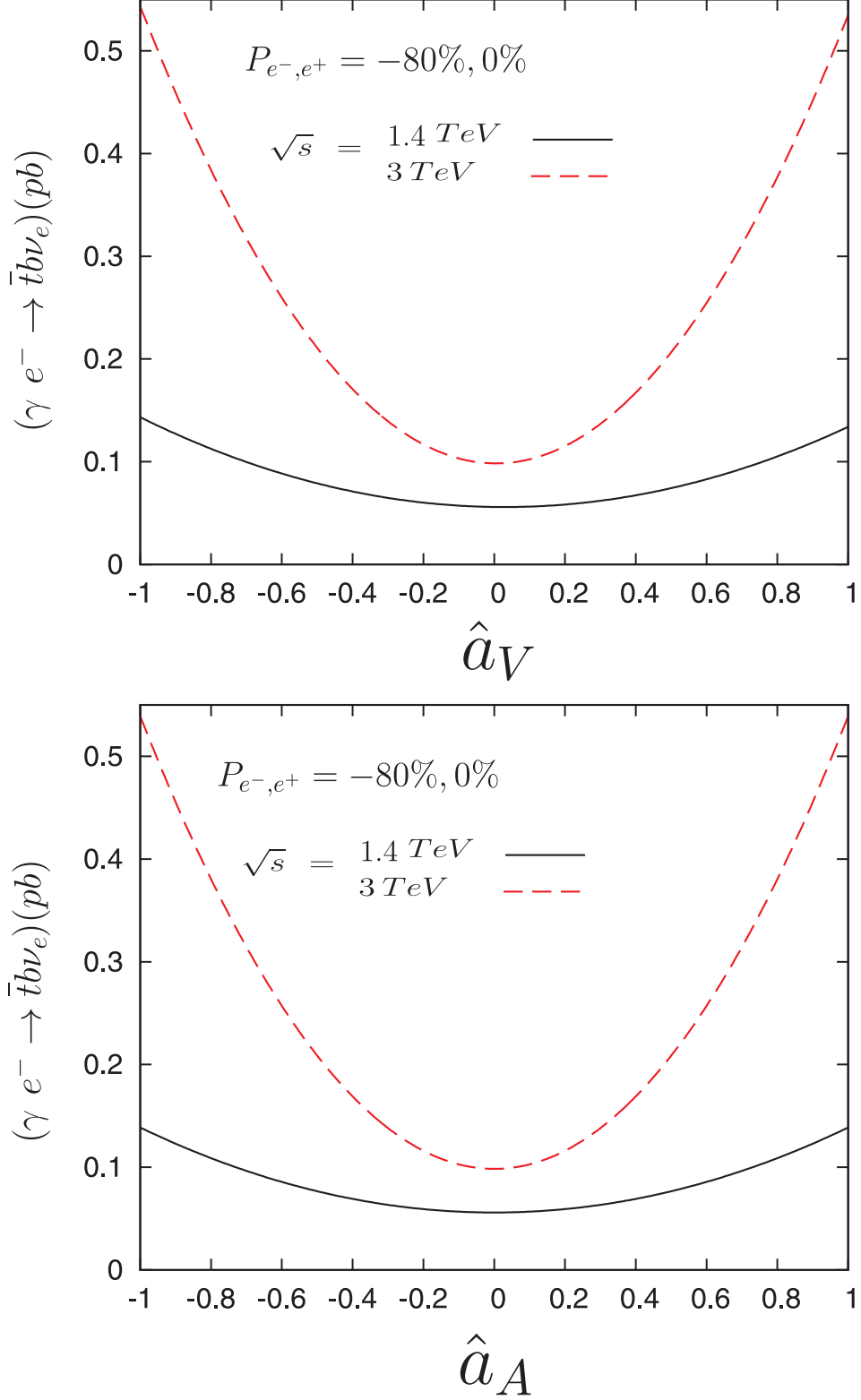


FIG. 3: The integrated total cross section of the process $\gamma e^- \rightarrow \bar{t} b \nu_e$ (γ is the Compton backscattering photon) as a function of \hat{a}_V and \hat{a}_A with $P_{e^-,e^+} = -80\%, 0\%$ and $\sqrt{s} = 1.4, 3 \text{ TeV}$, respectively.

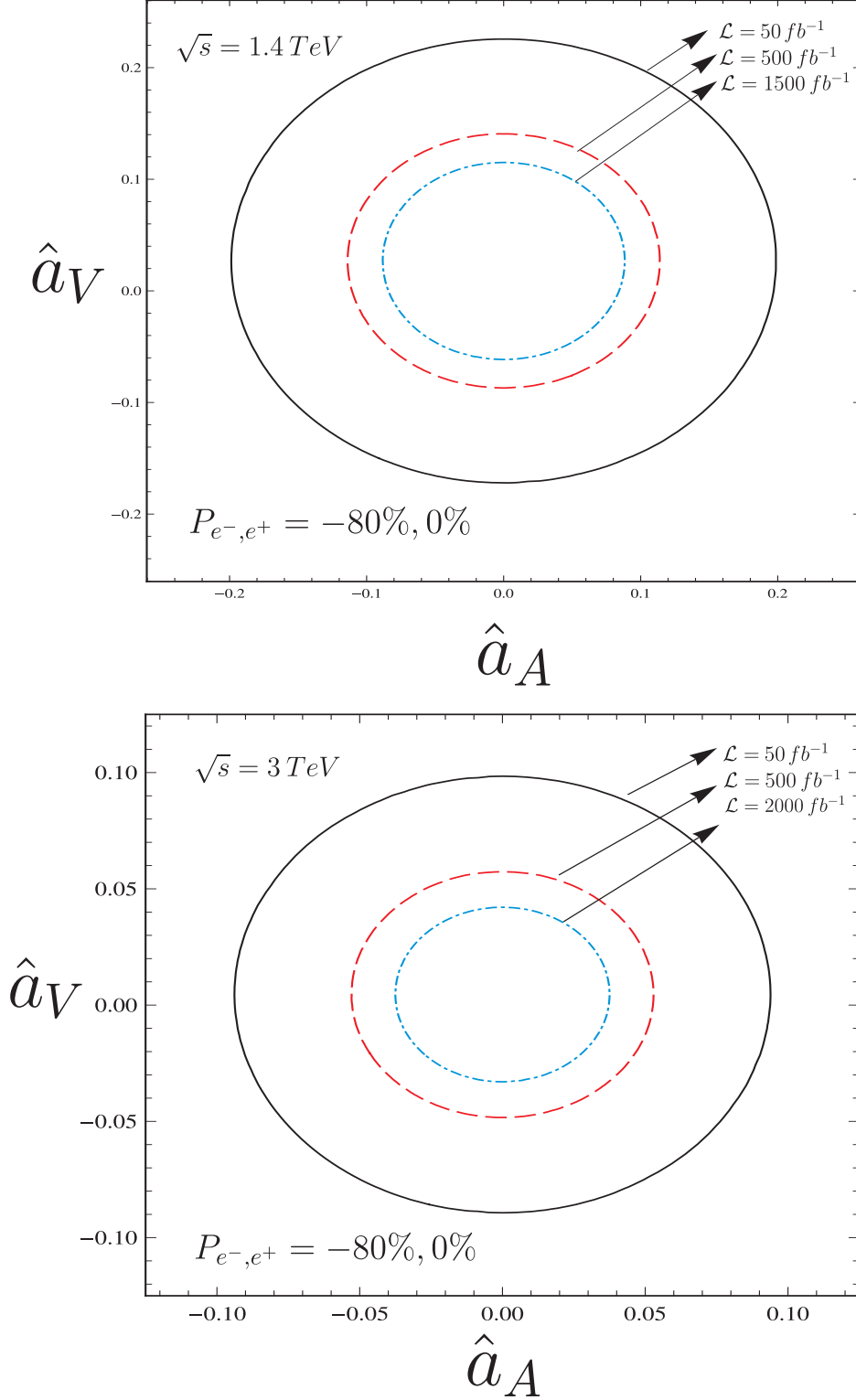


FIG. 4: Limits contours at the 95% *C.L.* in the $\hat{a}_V - \hat{a}_A$ plane for $\gamma e^- \rightarrow \bar{t} b \nu_e$ (γ is the Compton backscattering photon) with $P_{e^-,e^+} = -80\%, 0\%$ and $\sqrt{s} = 1.4, 3 \text{ TeV}$, respectively.

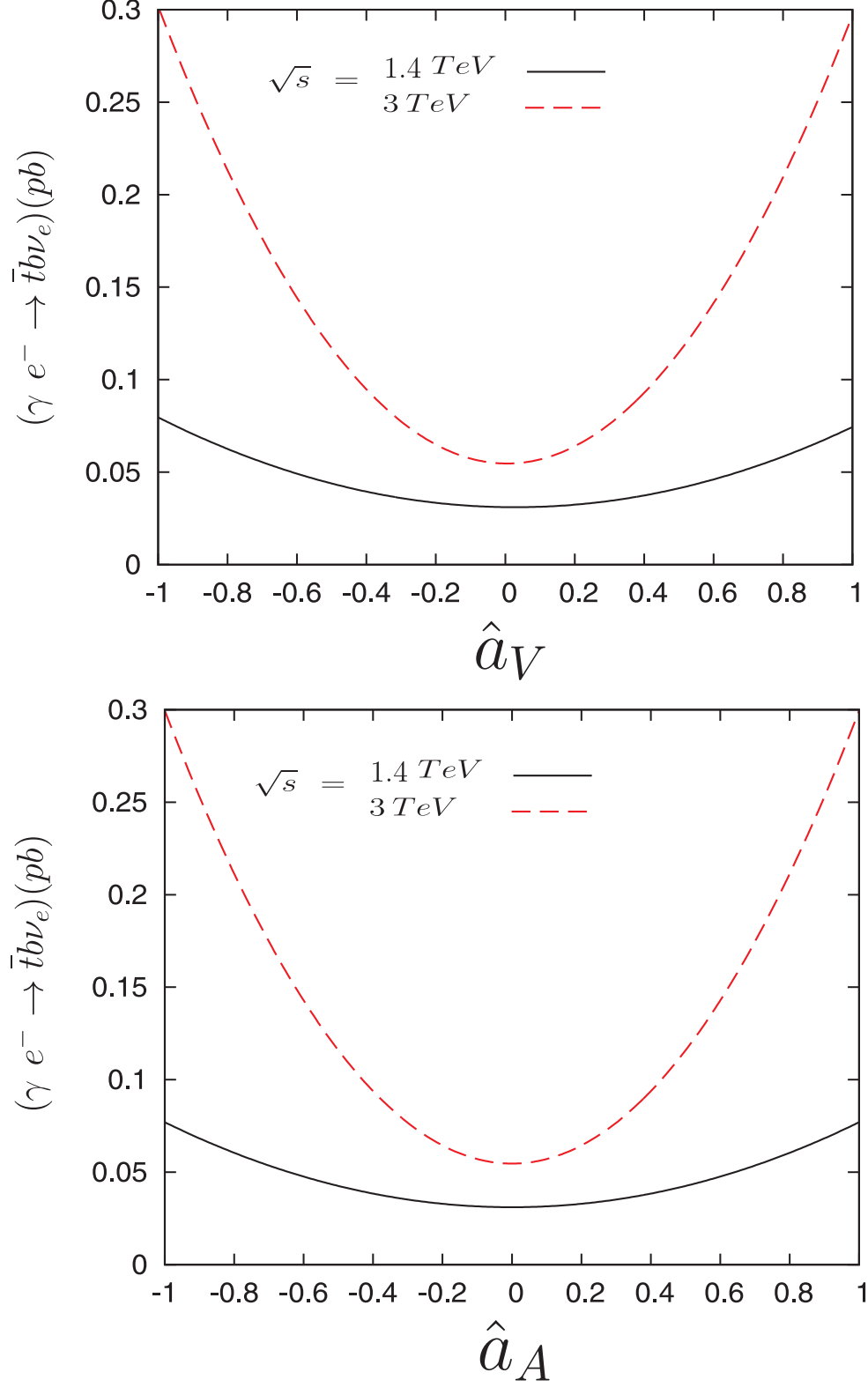


FIG. 5: The integrated total cross section of the process $\gamma e^- \rightarrow \bar{t} b \nu_e$ (γ is the Compton backscattering photon) as a function of \hat{a}_V and \hat{a}_A with $\sqrt{s} = 1.4, 3 \text{ TeV}$.

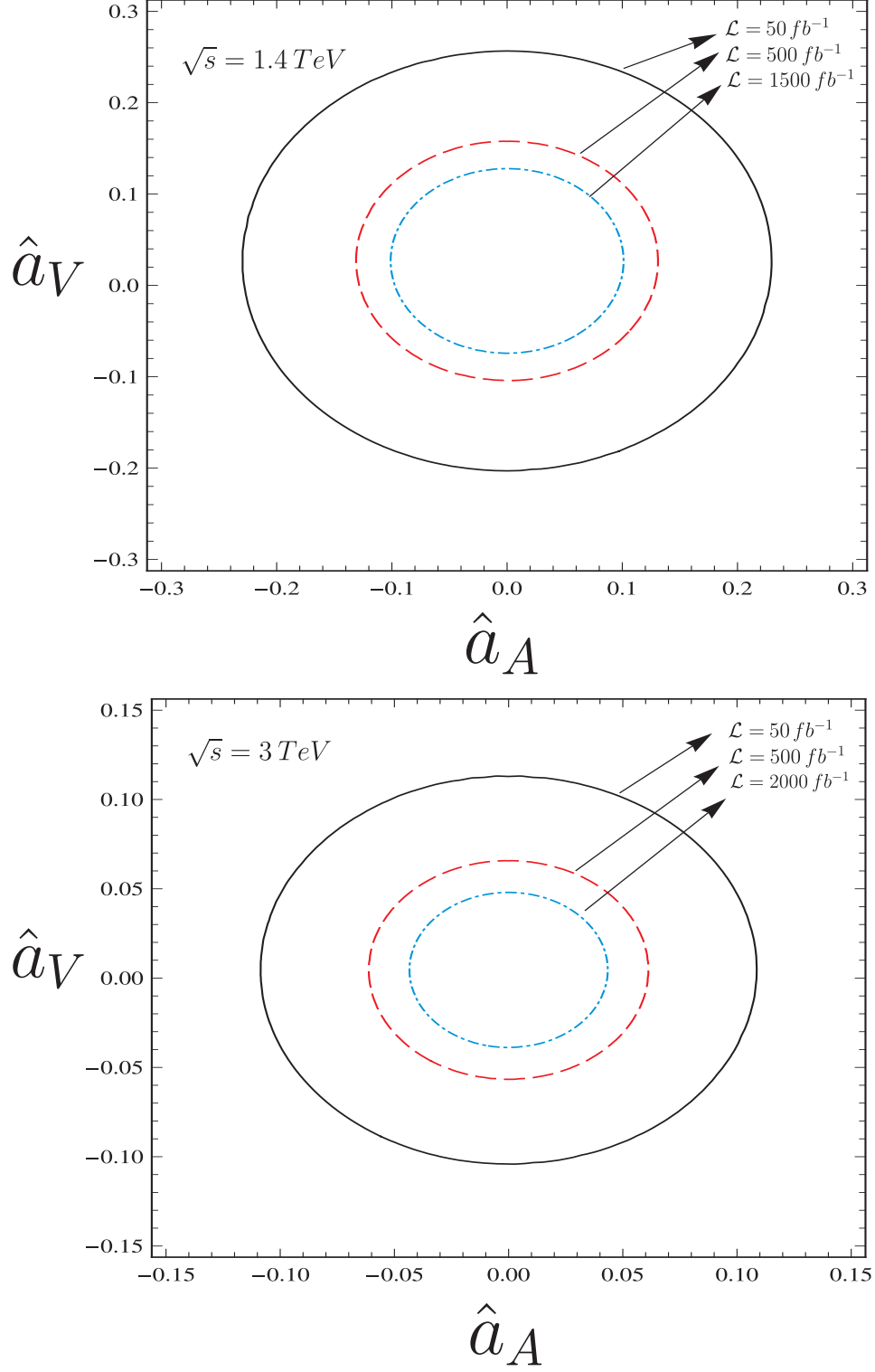


FIG. 6: Limits contours at the 95% *C.L.* in the \hat{a}_V - \hat{a}_A plane for $\gamma e^- \rightarrow \bar{t} b \nu_e$ (γ is the Compton backscattering photon) with $\sqrt{s} = 1.4, 3 \text{ TeV}$.

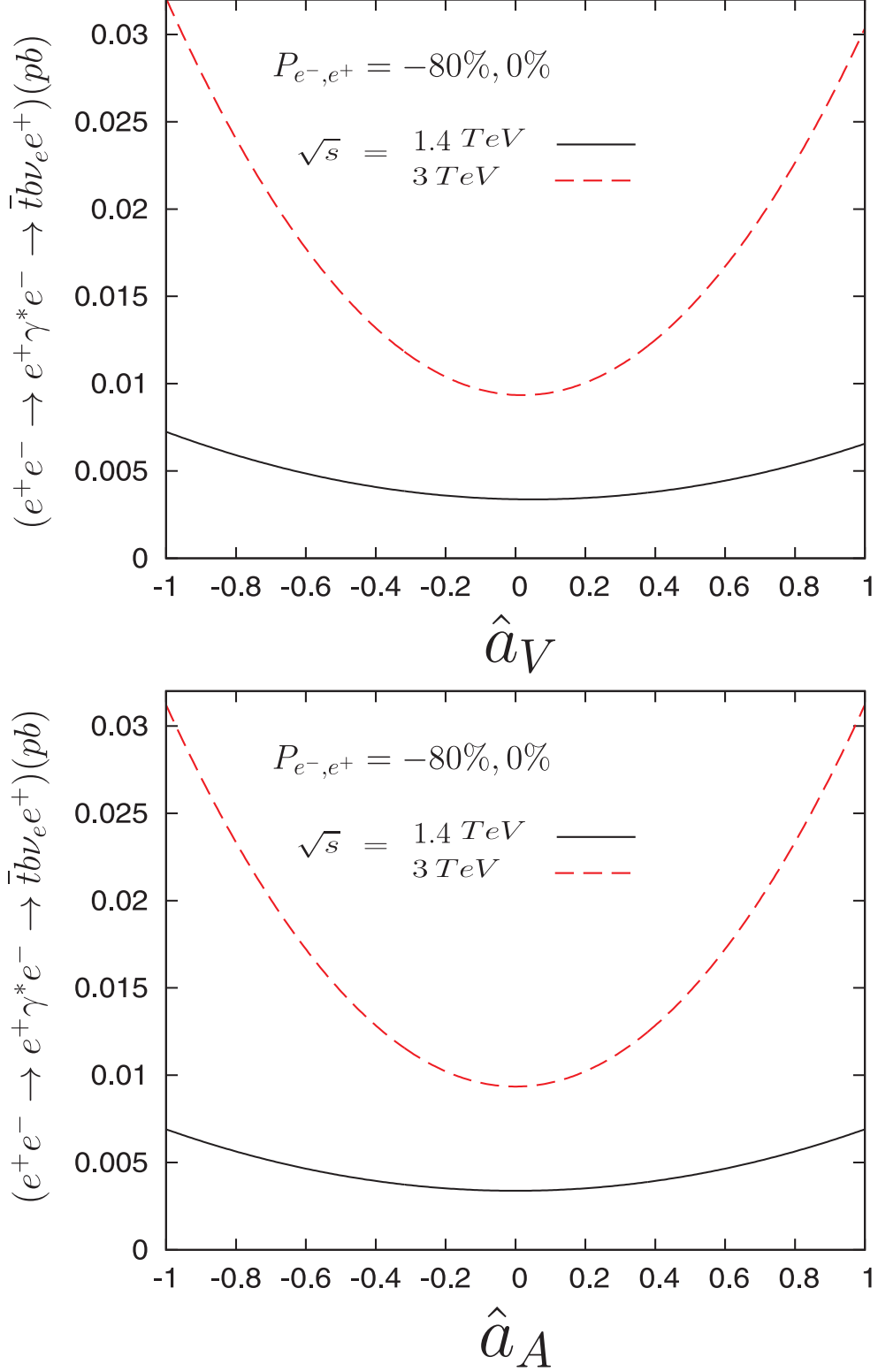


FIG. 7: The integrated total cross section of the process $e^+e^- \rightarrow e^+\gamma^*e^- \rightarrow \bar{t}b\nu_e e^+$ (γ^* is the Weizsacker-Williams photon) as a function of \hat{a}_V and \hat{a}_A with $P_{e^-,e^+} = -80\%, 0\%$, $\sqrt{s} = 1.4, 3 TeV$ and $Q^2 = 2 GeV^2$.

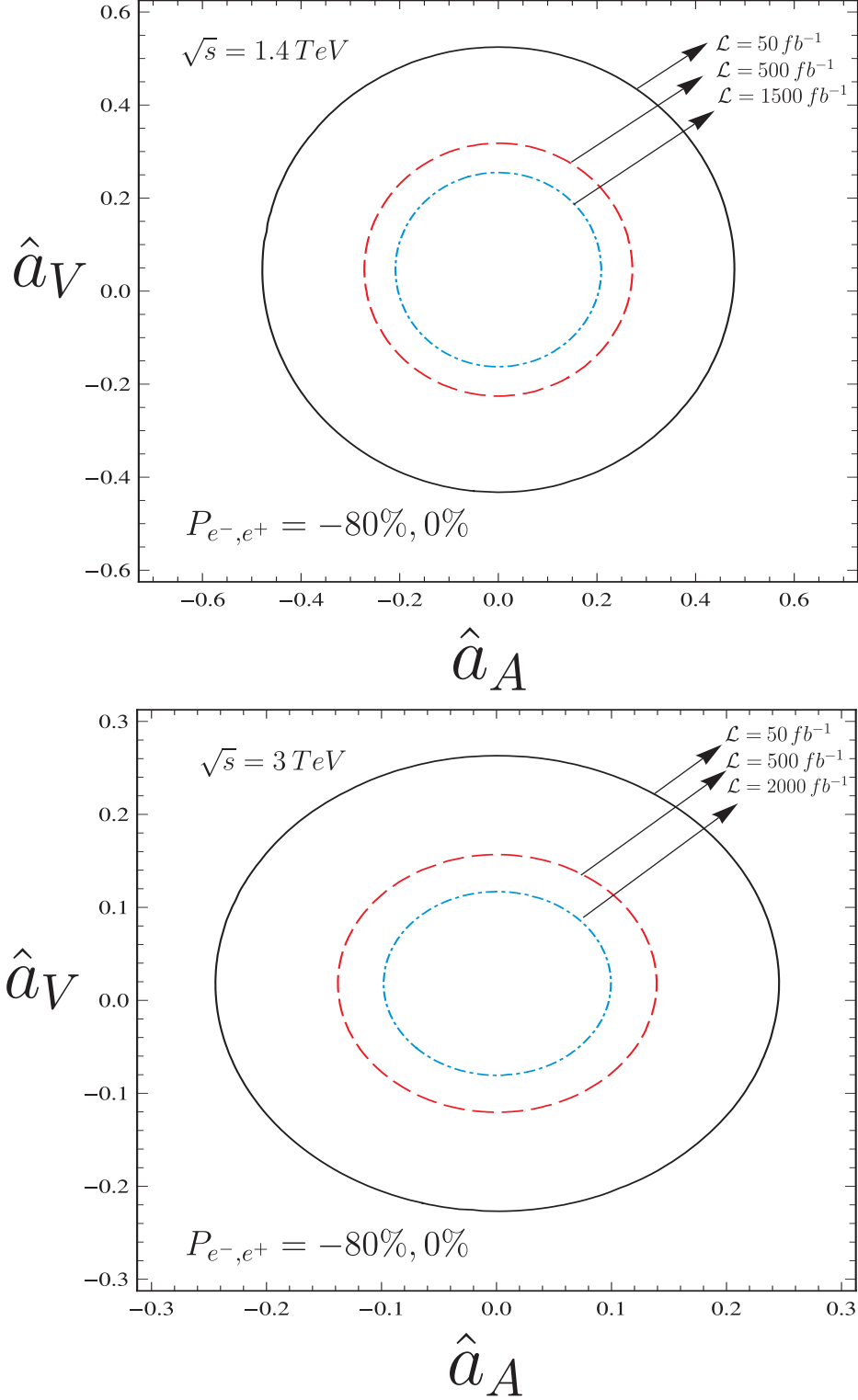


FIG. 8: Limits contours at the 95% *C.L.* in the \hat{a}_V - \hat{a}_A plane for $e^+e^- \rightarrow e^+\gamma^*e^- \rightarrow t\bar{b}\nu_e e^+$ (γ^* is the Weizsacker-Williams photon) with $P_{e^-,e^+} = -80\%, 0\%$, $\sqrt{s} = 1.4, 3 \text{ TeV}$ and $Q^2 = 2 \text{ GeV}^2$.

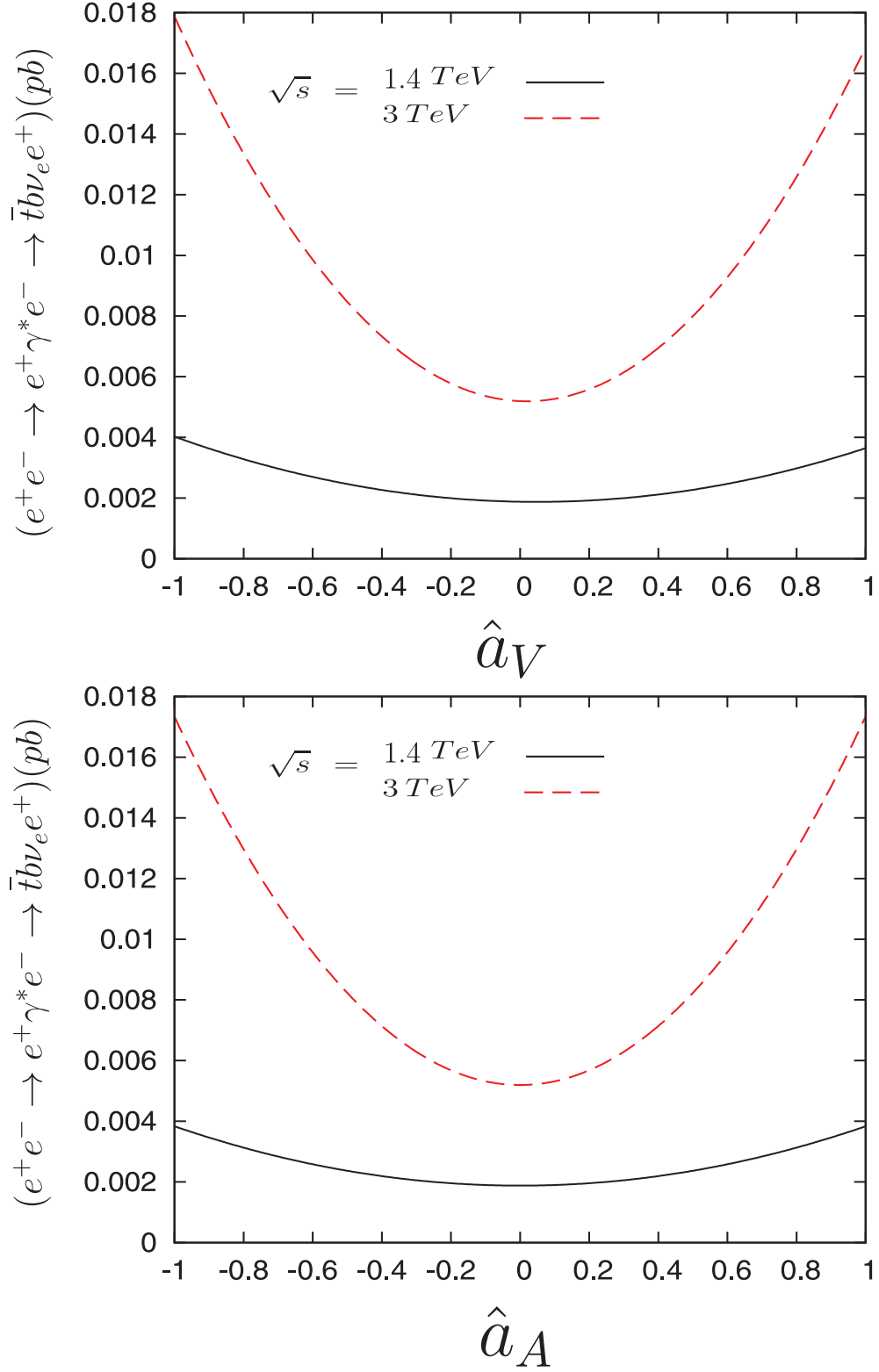


FIG. 9: The integrated total cross section of the process $e^+e^- \rightarrow e^+\gamma^*e^- \rightarrow \bar{t}b\nu_e e^+$ (γ^* is the Weizsacker-Williams photon) as a function of \hat{a}_V and \hat{a}_A with $\sqrt{s} = 1.4, 3 TeV$ and $Q^2 = 2 GeV^2$.

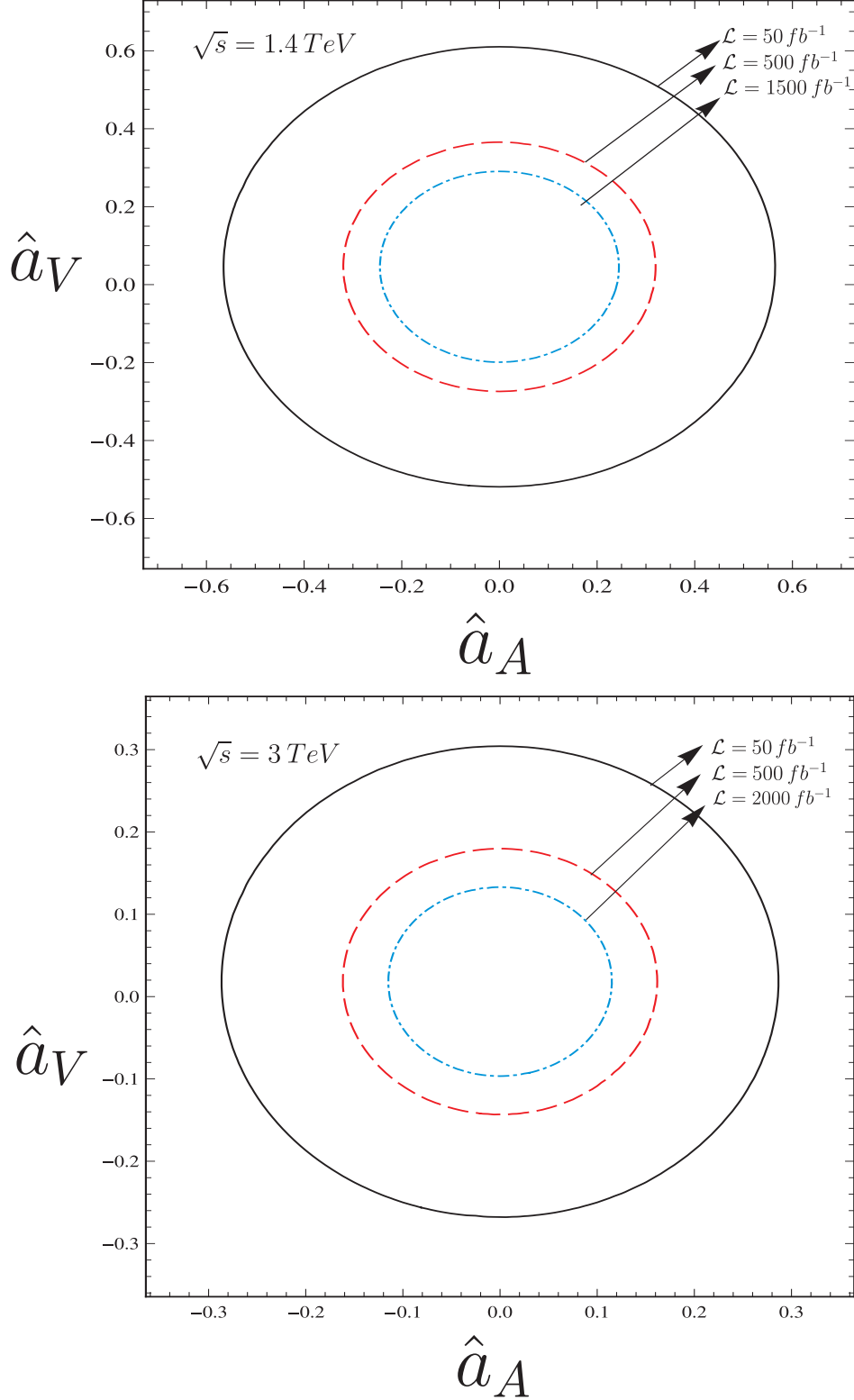


FIG. 10: Limits contours at the 95% *C.L.* in the \hat{a}_V - \hat{a}_A plane for $e^+e^- \rightarrow e^+\gamma^*e^- \rightarrow \bar{t}b\nu_e e^+$ (γ^* is the Weizsacker-Williams photon) with $\sqrt{s} = 1.4, 3 \text{ TeV}$ and $Q^2 = 2 \text{ GeV}^2$.